Dalton Transactions

PAPER

View Article Online
View Journal

Cite this: DOI: 10.1039/c9dt00554d

Carbon dioxide reduction by dinuclear Yb(II) and Sm(II) complexes supported by siloxide ligands†‡

Aurélien R. Willauer, [a] Davide Toniolo,[a] Farzaneh Fadaei-Tirani, [a] Yan Yang,[b] Maron Laurent [b] and Marinella Mazzanti *[a]

Received 5th February 2019,
Accepted 1st March 2019

DOI: 10.1039/c9dt00554d

rsc.li/dalton

Two dinuclear homoleptic complexes of lanthanides(II) supported by the polydentate tris(tertbutoxy) siloxide ligand ([Yb_2L_4], **1-Yb** and [Sm_2L_4], **1-Sm**, (L = $(O^tBu)_3SiO^-$)) were synthesized in 70–80% yield and **1-Sm** was crystallographically characterized. **1-Yb** and **1-Sm** are stable in solution at −40 °C but cleave the DME C–O bond over time at room temperature affording the crystal of [$Yb_2L_4(\mu\text{-}OMe)_2(DME)_2$], **2**. The **1-Yb** and **1-Sm** complexes effect the reduction of CO_2 under ambient conditions leading to carbonate and oxalate formation. The selectivity of the reduction towards oxalate or carbonate changes depend on the solvent polarity and on the nature of the ion. For both the lanthanides, carbonate formation is favoured but oxalate formation increases if a non-polar solvent is used. Computational studies suggest that the formation of oxalate is favoured with respect to carbonate formation in the reaction of the dimeric lanthanide complexes with CO_2. Crystals of the tetranuclear mixed-valence oxalate intermediate [$Yb_4L_8(C_2O_4)$], **3** were isolated from hexane and the presence of a $C_2O_4^{2-}$ ligand bridging two [$Yb^{II}L_2Yb^{III}L_2$] dinuclear moieties was shown. Crystals of the tetranuclear di-carbonate product [$Sm_4L_8(\mu_3\text{-}CO_3\text{-}\kappa^4\text{-}O,O',O'')_2$], **4** were isolated from hexane. The structures of **3** and **4** suggest that the CO_2 activation in non-polar solvents involves the interaction of two dimers with CO_2 molecules at least to some extent. Such a cooperative interaction results in both oxalate and carbonate formation.

Introduction

The potential application of CO_2 as a low-cost, widely available, abundant C1 feedstock for the synthesis of value-added organic compounds and fuels[1] has generated increasing interest towards the reduction of heteroallenes and other C1 substrates (such as CO) by f-element complexes.[2,3a,c,d,j,4,5]

The first example of CO_2 reduction by a lanthanide ion was reported by Evans more than twenty years ago. A Sm(II) biscyclopentadienyl complex ([$Cp^*_2Sm(thf)_2$]) was shown to promote the reductive coupling of CO_2 to afford selectively oxalate.[4j,6] Examples of reduction of CO_2 to oxalate remain rare both in d-[7] and f-block[3a,n,4h,j,6,8] metal chemistry. Moreover, oxalate formation is usually not selective and accompanied by the formation of other reduction or insertion products. Solvent effects were shown to play a key role in the outcome of the CO_2 reduction by d-block metal complexes.[7c] The importance of steric effects in determining the formation of oxalate *versus* carbonate formation in the reduction of CO_2 by mixed sandwich uranium(III) complexes incorporating a cyclo-pentadienyl ligand and a dianionic aromatic cyclooctatetraene was recently demonstrated in an elegant study by Cloke and coworkers.[8b] Cloke and coworkers also demonstrated, using a "harder" bisaryloxide supporting ligand, the importance of temperature and CO_2 pressure in determining the oxalate/carbonate ratio in CO_2 reduction by U(III) complexes.[4h]

In a related study on CO_2 reduction by mononuclear sandwich complexes of Sm(II), Nocton and coworkers showed the selective formation of carbonate and CO, when bulky cyclopentadienyl ligands are used as supporting ligands rather than Cp*, as a result of both steric and electronic effects.[9] A similar selectivity towards carbonate formation had been reported for the macrocyclic organosamarium(II) complex.[3d] In contrast, we showed previously that both oxalate and carbonate products were formed from the CO_2 reduction by an electron-rich mononuclear complex of Yb(II) supported by a polydentate tris(tertbutoxy) siloxide ligand.[8c]

These studies underline the important role that the nature of the metal and of the supporting ligand play in the CO_2 reduction.

[a]Institut des Sciences et Ingénierie Chimiques Ecole Polytechnique Fédérale de Lausanne (EPFL), 1015 Lausanne, Switzerland. E-mail: marinella.mazzanti@epfl.ch
[b]Université de Toulouse et CNRS INSA, UPS, CNRS, UMR 5215, LPCNO, 135 avenue de Rangueil, 31077 Toulouse, France

†Electronic supplementary information (ESI) available: Full computational and experimental details, NMR spectra, and detailed X-ray crystallographic data in CIF format. CCDC 1895385–1895388. For ESI and crystallographic data in CIF or other electronic format see DOI: 10.1039/c9dt00554d

‡Dedicated to Prof. Geoffrey Cloke, an inspiring scientist and a lovely man.

It has also become increasingly evident that another key parameter in the reduction of heteroallenes is the nuclearity of the metal complex. Notably, cooperative binding of heteroallenes by bimetallic complexes provides an attractive route for promoting their activation and reduction.[5g,10,11]

In most cases, the reduction of heteroallenes and other small molecules such as N_2, O_2, NO, or CO by f-elements involves two one-electron transfers by two metal complexes and results in dinuclear compounds where the two metals are bridged by the reduction product.[2b,3a,c,d,m,4a,j,g,5c,6,8b,12,13]

Computational studies corroborated the importance of bimetallic cooperativity in the reduction of heteroallenes by uranium and lanthanide complexes.[3h–j,l,n,5g,8d,14]

However, the use of polymetallic complexes of f-elements in the activation of small molecules is extremely rare[5f,8a,15] and only one example of a dinuclear complex able to reduce CO_2 has been reported for lanthanide ions. Notably, the dinitrogen complex $[\{(C_5Me_4H)_2Lu(THF)\}_2(N_2)]$ reacts with CO_2 affording selectively the oxalate bridged complex $[\{(C_5Me_4H)_2Lu\}_2(C_2O_4)]$.[8a,16]

Here we report two dinuclear complexes of lanthanides(II) supported by the polydentate tris(tertbutoxy)siloxide ligand ($[Yb_2L_4]$, **1-Yb** and $[Sm_2L_4]$, **1-Sm**, (L = $(O^tBu)_3SiO^-$)). We show that these complexes are able to reduce CO_2 in spite of the presence of only two electron-rich siloxide ligands and that the nature of the lanthanide ion, the solvent and the number of siloxide ligands play an important role in the ratio of oxalate *versus* carbonate formed in the reduction. Unprecedented tetranuclear Yb_2(II)Yb_2(III)-μ-C_2O_4 oxalate-bridged and Sm_4(III)(μ_3-CO_3-κ^4-O,O′,O″)$_2$ carbonate bridged complexes were isolated and crystallographically characterized.

It is remarkable that in the presence of dinuclear low coordinated metal complexes the CO_2 reduction involves more than two metal centres. Experimental and computational studies show that both intermolecular and intramolecular activation of carbon dioxide may occur in these dinuclear complexes.

Results and discussion

Syntheses of divalent lanthanide complexes

The divalent lanthanide complexes $[Yb_2L_4]$, **1-Yb** and $[Sm_2L_4]$, **1-Sm**, (L = $(O^tBu)_3SiO^-$) were obtained in 81% and 74% yield respectively, by treating $[Yb\{N(SiMe_3)_2\}_2(THF)_2]$ or $[Sm\{N(SiMe_3)_2\}_2(THF)_2]$ with two equivalents of $HOSi(O^tBu)_3$ in DME at −40 °C. Coordinated DME was removed completely by multiple recrystallizations of the reaction mixture residues from *n*-hexane (Scheme 1). Elemental analysis and ^{1}H NMR in Tol-d_8 and C_6D_{12} of the resulting solids confirmed the complete removal of DME. Crystals of **1-Sm** suitable for X-ray diffraction were obtained by storage of a concentrated *n*-hexane solution of the **1-Sm** complex at −40 °C.

The complex **1-Sm** crystallizes in the triclinic space group $P\bar{1}$. The structure of **1-Sm** is presented in Fig. 1 and shows the presence of a dimer where two lanthanide ions are bridged by three oxygen atoms from three different siloxide ligands. One

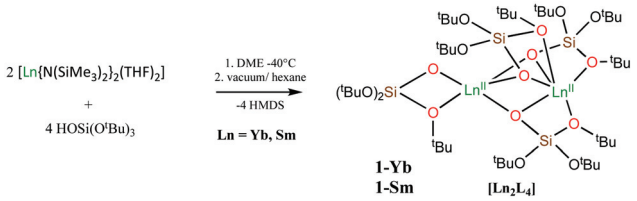

Scheme 1 Synthesis of complexes **1-Yb** and **1-Sm**.

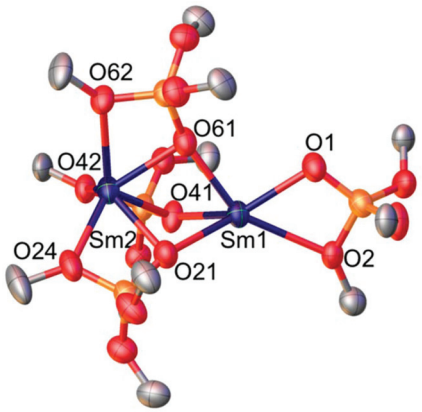

Fig. 1 Solid-state molecular structure of **1-Sm** (50% probability ellipsoids). Hydrogen atoms and methyl groups are omitted for clarity. Selected Sm–$O_{siloxide}$ bond lengths (Å): 2.387(5)–2.735(5).

lanthanide ion in the structure of **1-Sm** is five-coordinated by a terminal siloxide ligand in a bidentate fashion and by three bridging siloxides while the second metal ion is six-coordinated by three bridging siloxide ligands in a bidentate fashion. The crystal structure of the solvate complex $[Sm_2L_4(DME)]$,[17] was reported previously. The removal of the bound DME solvent from $[Sm_2L_4(DME)]$ does not result in a decreased stability of the resulting Sm(II) complex **1-Sm** because of the multiple coordination modes of the siloxide ligand. Notably, in both complexes the two Sm(II) ions show the same coordination number and in **1-Sm** the two DME oxygen donors are replaced by siloxide ones.

On the other hand, the Sm–$O_{siloxide}$ bond lengths in **1-Sm** fall in a slightly larger range (2.387(5)–2.735(5) Å) compared to the mononuclear $[SmL_4K_2]$ complex (2.381(2)–2.6659(18) Å)[8c] and the dimeric $[Sm_2L_4(dme)]$ complex (2.383(12)–2.692(13) Å).[17]

The complexes **1-Yb** and **1-Sm** are highly soluble in both polar and non-polar solvents. The ^{1}H NMR spectra at 25 °C of both complexes **1-Yb** and **1-Sm** in THF-d_8 show a single signal for all siloxide ligands in agreement with the presence of fluxional species and solvent binding. The ^{1}H NMR spectrum of **1-Yb** in Tol-d_8 and C_6D_{12} at 25 °C shows a single narrow signal corresponding to the 108 protons of the siloxide ligands in agreement with the presence of fluxional species in solution. The ^{1}H NMR spectrum of **1-Sm** at 25 °C shows one broad signal in Tol-d_8 and two signals in C_6D_{12} corresponding to the 108 protons of the siloxide ligands suggesting a reduced flux-

ionality of the samarium species in solution. The ^{1}H NMR spectrum of **1-Yb** in Tol-d_8 at −60 °C shows also the presence of two signals in agreement with the presence of similar solution species compared to **1-Sm** but higher fluxionality. The presence of the dimeric complex **1-Yb** in C_6D_{12} solution was confirmed by DOSY NMR spectroscopy. The value of the molecular diameter measured for **1-Yb** (12.7 Å) was found to be consistent with the value estimated from the solid-state structure of **1-Sm** (12 Å).

Although **1-Yb** and **1-Sm** are stable in the solid state and in solution at −40 °C, ^{1}H NMR studies indicated a lower stability in solution at room temperature showing evidence of decomposition in THF and in toluene after 36 h. Notably, a decrease of the ^{1}H NMR signal assigned to the siloxide ligands is observed over time for both **1-Yb** and **1-Sm**.

The complex [Sm_2L_4(DME)] was previously shown to slowly react at room temperature with toluene affording, after a few days, the tetranuclear divalent samarium sandwich complex [{Sm_2L_3}$_2$(μ-η^6:η^6-C_7H_8)].[17] The spectroscopic ^{1}H NMR study of **1-Sm** in Tol-d_8 at room temperature shows that the removal of the DME molecule from the coordination environment of the samarium metal centre does not impact the formation of this multiple decker complex. Notably, the ^{1}H NMR spectra of **1-Sm** in Tol-d_8 over time show the appearance after 5 days of a signal at δ = 1.08 ppm assigned to the complex [{Sm_2L_3}$_2$(μ-η^6:η^6-C_7H_8)].[17] The complex **1-Yb** also decomposes in toluene but we were not able to isolate the reaction products.

The complex **1-Yb** also reacts with DME over time at room temperature. After 3 weeks at room temperature, highly insoluble colourless crystals of [Yb_2L_4(μ-OMe)$_2$(DME)$_2$], **2**, were isolated in low yield (Scheme 2). The complex **2** crystallizes in the triclinic space group $P\bar{1}$ and is presented in Fig. 2. The centrosymmetric structure features a trivalent binuclear ytterbium complex with six-coordinated metal ions. Each ytterbium ion is coordinated by two siloxide ligands in a k^1 fashion, a k^2-DME molecule and two μ$_2$–κ^1-methoxy groups. The Yb–$O_{siloxide}$ distances are consistent with values reported for Yb^{III} tris(*tert*-butoxy)siloxide ligands.[8c,18]

The cleavage of the C–O bond in DME by divalent ytterbium complexes has been observed previously in the litterature.[19] The Yb–O3A distances (2.205(4) and 2.272(4) Å) in **2** are similar to the Yb–OMe distances in the analogous complexes [Yb_2I_4(μ-OMe)$_2$(DME)$_2$] (2.152(4) and 2.210(6) Å),[19a] [Yb_2(N(SiMe$_3$)C$_6$H$_4$-2-OMe)$_4$(μ-OMe)$_2$] (2.217(2) and 2.221(2) Å),[19c] and [Yb_2(OAr)$_4$(μ-OMe)$_2$(DME)$_2$] (2.191(2) and 2.258(2) Å).[19b]

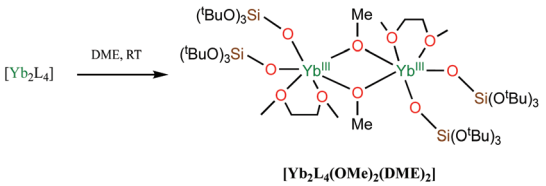

Scheme 2 Decomposition of **1-Yb** in DME at room temperature.

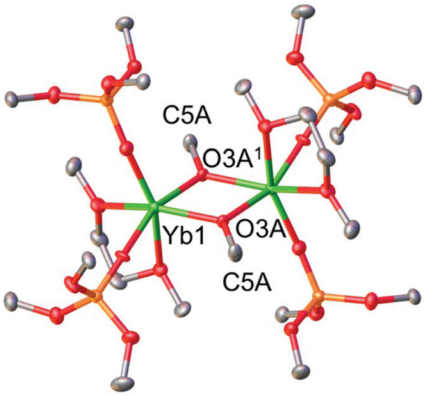

Fig. 2 Solid-state molecular structure of **2** (50% probability ellipsoids). Hydrogen atoms and methyl groups from ^{t}Bu are omitted for clarity. Selected bond lengths (Å): Yb–$O_{siloxide}$ = 2.101(4)–2.125(4); Yb1–O3A = 2.205(4); Yb1–O3A^1 = 2.272(4); O3A–C5A = 1.430(7). Symmetry transformation used to generate equivalent atoms: ^{1}1 − *x*, 1 − *y*, 1 − *z*.

The moderate stability of complexes **1-Yb** and **1-Sm** in Tol-d_8, DME and THF-d_8 prompted us to investigate their stability in cyclohexane at room temperature. The ^{1}H NMR spectra of the solutions of **1-Yb** and **1-Sm** in C_6D_{12} did not show any decrease of the area of the signals, highlighting their stability for weeks in C_6D_{12} at room temperature.

Reactivity with carbon dioxide

In previous studies we reported the synthesis and structure of the mononuclear homoleptic complexes [Ln^{II}(OSi(O^{t}Bu)$_3$)$_4$K$_2$] ([LnL$_4$K$_2$]) for Sm, Eu and Yb. The presence of four electron-rich tris(*tert*-butoxy)siloxide ligands imparts stability and unusual reactivity to the metal center leading to the first example of CS_2 and CO_2 activation by a Yb(II) complex. Notably, [YbL$_4$K$_2$], reacts with CO_2 affording quantitatively oxalate and carbonate in the ratio 1 : 2.2 and CO. However, the bulky siloxide ligands enforce the labile binding of the reduction products preventing the isolation of reaction intermediates where the substrate or reduction products are metal-bound.

In the dinuclear complexes **1-Yb** and **1-Sm** the presence of only two tris(*tert*-butoxy)siloxide ligands should allow the isolation of reaction intermediates. However, the presence of only two siloxide ligands will result in an overall lower reducing power of the **1-Yb** and **1-Sm** complexes compared to the ate analogues [YbL$_4$K$_2$] and [SmL$_4$K$_2$] that could prevent CO_2 reduction. Indeed, the reactivity of Ln(II) complexes is ligand dependent[20] and it was recently shown, that the dinuclear, neutral, low coordinated [Sm^{II}(OTf)$_2$(DME)$_2$]$_2$ complex[15d] does not reduce carbon dioxide in contrast with reports describing CO_2 reduction by neutral Sm(II) complexes supported by Cp,[4j,9] or porphyrinogen ligands.[3d]

In order to understand how the number of siloxide ligands and the complex nuclearity affect the reduction of CO_2 by divalent lanthanides we investigated the reactivity of **1-Yb** and **1-Sm** with CO_2. **1-Yb** and **1-Sm** react immediately with CO_2 at

room temperature affording CO and carbonate or oxalate. However, the ratio between carbonate and oxalate is different for **1-Yb** and **1-Sm** compared to $[YbL_4K_2]$ and $[SmL_4K_2]$ in the same solvent. Moreover, the carbonate : oxalate ratio was found to vary depending on the solvent and the lanthanide ions (Table 1).

When $^{13}CO_2$ (~5 equivalents) was added to a THF-d_8 solution of **1-Yb**, an immediate colour change was observed from orange to yellow (Scheme 3). The ^{1}H NMR spectrum of the reaction mixture in THF-d_8, recorded immediately after addition, shows the complete disappearance of the signal assigned to **1-Yb** and the appearance of new signals. A signal assigned to the trivalent species $[YbL_3(THF)_2]$ (δ = −16.93 ppm) increases over time reaching approximately 50% yield after 10 days. These data suggest that mononuclear Yb(III) complexes containing bound reduction products are also present in the solution.

The ^{13}C NMR spectrum of the reaction mixture in THF-d_8 shows the presence of free ^{13}CO and $^{13}CO_2$ as well as a signal at δ = 169.95 ppm that was assigned to the bound carbonate product. No change in the ^{13}C NMR spectrum could be detected over time. The quantitative ^{13}C NMR spectrum of the residue (after removal of the solvent) in basic (pD = 13) deuterated water confirmed the presence of carbonate (δ = 168.26 ppm) as the single product of carbon dioxide reduction in 90% yield.

When $^{13}CO_2$ (~5 equivalents) was added to a C_6D_{12} solution of **1-Yb** an immediate colour change was observed from brown to yellow (Scheme 4). The ^{1}H NMR spectrum in C_6D_{12} of the reaction mixture, immediately after the addition of $^{13}CO_2$, showed the appearance of three new signals and unreacted **1-Yb**. After three days, the ^{1}H NMR spectrum showed the complete disappearance of **1-Yb**.

The ^{13}C NMR spectrum after two weeks shows only excess CO_2. The solvent and the excess $^{13}CO_2$ were removed and the residue was dissolved in deuterated water at pD = 13 in order to release the products of carbon dioxide reduction from the ytterbium metal centres. A very basic pD is required to release completely the bound oxalate and carbonate. The quantitative ^{13}C NMR spectrum showed the presence of carbonate (δ = 167.62 ppm) and oxalate (δ = 179.72 ppm) in a ratio of 50 : 1 with 94% total yield (carbonate + oxalate).

These results show that in THF the reduction of CO_2 by **1-Yb** only leads to the formation of carbonate, but oxalate is also formed when a non-polar solvent is used. Compared to the tetra-siloxide $[YbL_4K_2]$ complex (ratio oxalate : carbonate 1 : 2.2),[8c] the bis-siloxide, **1-Yb**, leads to a higher selectivity for carbonate formation probably as a result of lower steric hindrance at the metal centre. In the reaction of $[YbL_4K_2]$ with CO_2 the reduction products are rapidly released and it was impossible to isolate intermediates.[8c] Attempts to isolate the Yb-bound carbonate species from THF or hexane solutions were also unsuccessful probably due to the presence of multiple products (only single crystals of $[YbL_3(THF)_2]$ could be isolated).

However, overnight storage at −40 °C of a concentrated hexane solution of the reaction mixture obtained after the reaction of **1-Yb** with ~5 equivalents CO_2 at room temperature performed in C_6D_{12} allowed the isolation of crystals suitable for X-ray diffraction of the tetranuclear mixed-valence complex $[Yb_4L_8(C_2O_4)]$, **3** (Fig. 3). The complex **3** crystallizes in the tri-

Table 1 Oxalate : carbonate molar ratios from the reaction of $[Ln_2L_4]$ (Ln = Yb, Sm, 25 mM) and $[LnL_4K_2]$ (Ln = Yb, Sm, 25 mM) with CO_2 after the release of the CO_2 reduction products in basic (pD = 12–13) water

Reagents	Solvent	$C_2O_4^{2-}$: CO_3^{2-}
$[Yb_2L_4]$	THF-d_8	0 : 1
$[YbL_4K_2]$	THF-d_8	1 : 3
$[Yb_2L_4]$	C_6D_{12}	1 : 50
$[YbL_4K_2]$	Tol-d_8	1 : 1.5
$[Sm_2L_4]$	THF-d_8	1 : 104
$[Sm_2L_4]$	C_6D_{12}	1 : 17
$[SmL_4K_2]$	C_6D_{12}	1 : 0.8
$[SmL_4K_2]$	Tol-d_8	1 : 0.8

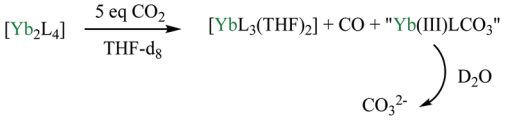

Scheme 3 Reaction of **1-Yb** with carbon dioxide in THF-d_8.

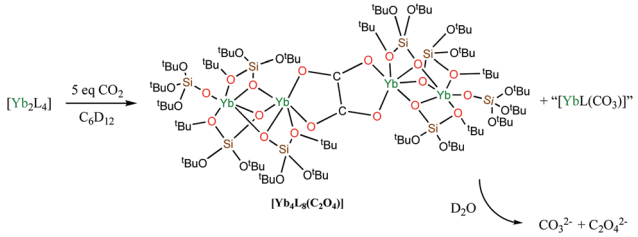

Scheme 4 Reaction of $[Yb_2L_4]$, **1-Yb**, with carbon dioxide in cyclohexane.

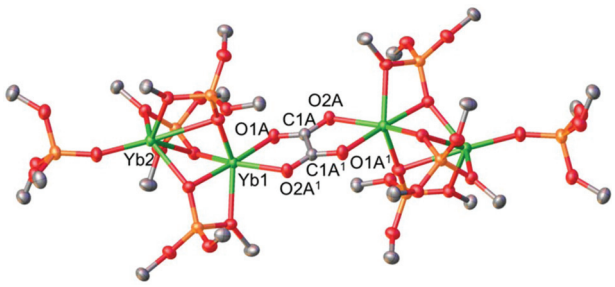

Fig. 3 Solid-state molecular structure of **3** (50% probability ellipsoids). Hydrogen atoms and methyl groups were omitted for clarity. Selected bond lengths (Å): Yb1–$O_{siloxide}$ = 2.0945(12)–2.3649(12); Yb2–$O_{siloxide}$ = 2.2143(12)–2.7426(14); Yb1–O1A = 2.2993(13); Yb1–$O2A^1$ = 2.3025(13); O1A–C1A = 1.256(2); O2A–C1A = 1.251(2); C1A–$C1A^1$ = 1.554(3). Symmetry transformation used to generate equivalent atoms: ^{1}1 − *x*, 1 − *y*, 1 − *z*.

clinic space group $P\bar{1}$ as a tetramer. The solid-state structure shows the presence of a $C_2O_4^{2-}$ ligand bridging two $[Yb^{II}L_2Yb^{III}L_2]$ dinuclear moieties. The two moieties are composed of two six-coordinated ytterbium ions. The first ytterbium is coordinated to one terminal k^1-siloxide ligand, two bridging k^2-siloxide ligands and one bridging k^1-siloxide ligand. The second ytterbium metal center is coordinated to one bridging k^2-siloxide ligand, two bridging k^1-siloxide ligands and one k^2-C_2O_4 ligand. The Yb1–$O_{siloxide}$ (2.0945(12)–2.3649(12) Å) distances and the Yb2–$O_{siloxide}$ (2.2143(12)–2.7426(14) Å) distances fall in the range of Yb^{III}–$O_{siloxide}$ (2.029(3)–2.339(2) Å)[18] and Yb^{II}–$O_{siloxide}$ distances (2.251(6)–2.571(6) Å),[8c] respectively, in agreement with the presence of mixed-valence $[Yb^{II}L_2Yb^{III}L_2]$ dimeric moieties. The C1A–C1A^1 bond length is 1.554(3) Å which is consistent with the formation of a single C–C bond (1.54 Å in ethane). The isolation of complex **3** suggests that two complexes **1-Yb** interact with two CO_2 molecules in their dinuclear form when the reaction is carried out in a non-coordinating solvent. However, only one of the Yb(II) centers in **1-Yb** transfers one electron to the CO_2 molecule while the second Yb center remains in the oxidation state + II probably due to its lowered redox potential in the presence of the Yb(III) ion. Thus, two Yb(II) centers from two dinuclear complexes transfer one electron to two CO_2 molecules resulting in their reductive coupling to oxalate. The dinuclear form seems to favour the oxalate formation. Notably when the reaction is carried out in THF, a coordinating-solvent, where the complex **1-Yb** is likely to adopt a mononuclear form,[21] only carbonate is formed. This may be due both to the electronic and steric differences at the Yb(II) center in **1-Yb** and in the mononuclear analogue $[Yb^{II}L_2(THF)x]$.

The high yield in oxalate + carbonate (94%) indicates that complex **3** is a moderately stable intermediate that must react further with CO_2 to afford additional reduction products. Indeed, once the reaction is complete, all Yb(II) complexes have reacted to afford oxalate or carbonate reduction products.

In order to assess the influence of the nature of the lanthanide ion on the reactivity we also investigated the reactivity of **1-Sm**.

The reaction of $[Sm_2L_4]$, **1-Sm** with $^{13}CO_2$ (~5 equivalents) in THF-d_8 afforded a colour change from dark brown to colourless over few minutes (Scheme 5). The ^{1}H NMR spectrum of the reaction mixture in THF-d_8, immediately after the addition, shows the complete disappearance of the signal assigned to **1-Sm** and the apparition of signals assigned to $[SmL_3(THF)_2]$. The signals continuously increased over two days, reaching approximately 50% yield for $[SmL_3(THF)_2]$. The ^{13}C NMR spectrum in THF-d_8 shows the presence of free ^{13}CO and $^{13}CO_2$ as well as new signals at δ = 174.61 ppm and 174.38 ppm that shift over time.

The solvent and the excess $^{13}CO_2$ were removed after two days and the residue was dissolved in basic (pD = 13) deuterated water. The quantitative ^{13}C NMR spectrum in D_2O showed the presence of carbonate and oxalate in a 104 : 1 ratio and in 90% total yield (carbonate and oxalate).

These results indicate that while in THF the reduction of CO_2 by **1-Yb** only leads to the formation of carbonate, the reduction of CO_2 by **1-Sm** also leads to the formation of a low amount of oxalate. No intermediate Sm(II) complexes containing bound carbonate or carboxylate could be isolated from THF.

The reaction of $[Sm_2L_4]$, **1-Sm** with $^{13}CO_2$ (~5 equivalents) in C_6D_{12} afforded a less radical colour change, compared to THF-d_8, from dark brown to light brown (Scheme 6). The ^{1}H NMR spectrum of the reaction mixture in C_6D_{12} shows the immediate disappearance of **1-Sm** and the appearance of new signals. The ^{13}C NMR spectrum in C_6D_{12} shows the presence of $^{13}CO_2$ in excess and free ^{13}CO as well as the presence of additional signals assigned to Sm-bound CO_2 reduction products. After four days at room temperature the solution turned colourless. The broad ^{1}H NMR spectrum did not show any detectable change over time, but important changes were observed in the number and chemical shift of the ^{13}C NMR signals over time. These changes may be due to the presence of detectable intermediate CO_2 reduction products or to changes occurring over time in the binding mode of the CO_2 reduction products to the Sm complex. The quantitative ^{13}C NMR spectrum of the reaction mixture in basic (pD = 13) D_2O after 10 days showed the presence of oxalate and carbonate in a 1 : 17 ratio and in 98% total yield.

These results indicate that the reduction of CO_2 by **1-Sm** in C_6D_{12} leads to higher amounts of oxalate compared to the reduction in THF-d_8 or to the reduction of CO_2 by **1-Yb** in THF or C_6D_{12} but no intermediate containing bound oxalate could be isolated.

In contrast, storage for 2 days at −40 °C of a concentrated hexane solution of **1-Sm** after reaction with $^{13}CO_2$ (~5 equivalents) in C_6D_{12} at room temperature allowed the isolation of X-ray diffraction suitable crystals of $[Sm_4L_8(\mu_3\text{-}CO_3\text{-}\kappa^4\text{-}O,O',O'')_2]$, **4**. The molecular structure of **4** (Fig. 4) shows the presence of a Sm(III) tetrameric complex where each metal center is

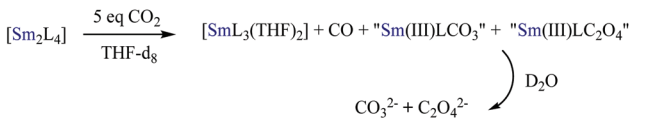

Scheme 5 Reaction of $[Sm_2L_4]$, **1-Sm**, with carbon dioxide in THF-d_8.

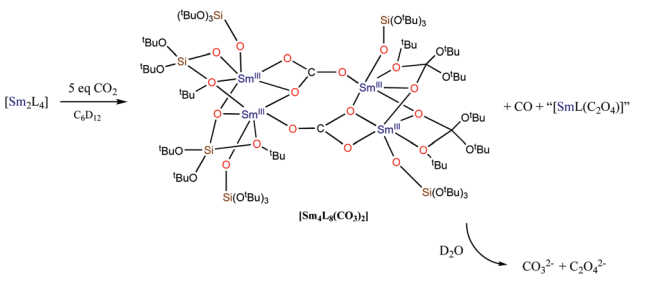

Scheme 6 Reaction of $[Sm_2L_4]$, **1-Sm**, with carbon dioxide in cyclohexane.

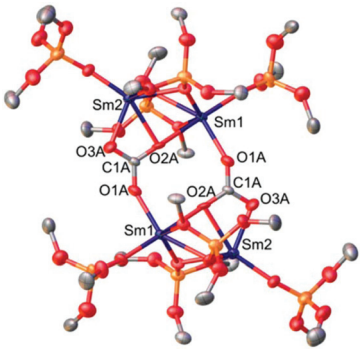

Fig. 4 Solid-state molecular structure of **4** (50% probability ellipsoids). Hydrogen atoms and methyl groups were omitted for clarity. Selected bond lengths (Å): Sm–$O_{siloxide}$ = 2.150(6)–2. 479(6); Sm1–O1A = 2.258(7); Sm1–O2A[1] = 2.420(7); Sm2–O2A = 2.485(6); Sm2–03A = 2.295(7); C1A–O = 1.274(10)–1.287(11). Symmetry transformation used to generate equivalent atoms: [1]3/2 − *x*, 1/2 − *y*, 1 − *z*.

six-coordinated. The dimer is built from two identical $[Sm_2L_2(\mu\text{-}L)_2]$ moieties each composed of two samarium(III) ions coordinated to one terminal siloxide ligand in a k^1 fashion, one bridging k^1-siloxide ligand and one bridging k^2-siloxide ligand. The two $[Sm_2L_2(\mu\text{-}L)_2]$ moieties are bridged by two carbonate groups in a μ_3-κ^4-O,O′,O″ fashion. The Sm–$O_{siloxide}$ distances (2.150(6)–2. 479(6) Å) are similar to those found in the previously reported Sm(III) complexes.[22] A similar tetranuclear carbonate Sm(III) complex was reported very recently using triflate as the supporting ligand ($[Sm_4(CO_3)_2(OTf)_8(THF)_{10}]$).[15d] However, the Sm(II) precursor $[Sm(OTf)_2(DME)_2]$ did not react directly with CO_2 but only *via* the formation of a oxo complex of Sm(III) after the reaction with a O-transfer agent. The carbonate C–O distances (1.274(10)–1.287(11) Å) and the O–C–O angles (117.3(8)–122.2 (8)°) in **4** are similar to those found in the samarium triflate complex (1.263(2)–1.315(2) Å and 115.8(2)–125.1(2)°). Furthermore, the Sm–$O_{carbonate}$ bond lengths are in the range of previously reported trivalent samarium carbonate complexes.[9,15d]

In order to compare the reactivity with carbon dioxide between the bis-siloxide complex **1-Sm** and the previously reported tetra-siloxide $[SmL_4K_2]$ complex, the reaction of $[SmL_4K_2]$ with $^{13}CO_2$ (~5 equivalents) in C_6D_{12} was performed (Scheme 7). This afforded a color change of the solution from red to colourless. ^{1}H NMR spectroscopy studies showed the complete disappearance of the signal assigned to $[SmL_4K_2]$ and the appearance of a single signal at δ = 0.55 ppm corresponding to the trivalent species $[SmL_4K]$ in approximately 50% yield, determined by NMR using naphthalene as the internal

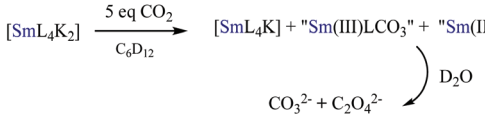

Scheme 7 Reaction of $[SmL_4K_2]$, with carbon dioxide in cyclohexane.

standard. The ^{13}C NMR spectrum in C_6D_{12} shows the formation of new signals assigned to Sm-bound reduced CO_2 species. No evolution in the ^{1}H NMR or ^{13}C NMR spectra could be observed suggesting a faster reaction compared to **1-Sm**.

The quantitative ^{13}C NMR spectrum in basic D_2O (pD = 12) showed the presence of oxalate (δ = 173.36 ppm) and carbonate (δ = 168.22 ppm) in a ratio of 1 : 0.8 and in 92% total yield (carbonate and oxalate). The same ratio was observed when the reaction was performed in Tol-d_8.

These results indicate that the use of the bulkier tetra-siloxide $[SmL_4K_2]$ complex leads to the formation of the oxalate in a higher yield compared to **1-Sm**, becoming the major product of CO_2 reduction.

Computational studies

DFT calculations were carried out in order to determine possible reaction pathways and to explain the observed trend of product formation. Previous studies on Sm(II) catalyzed CO_2 reduction[3d,9] have demonstrated that carbonates are formed, that are kinetic products, while others[3h,n,4j] reported the formation of oxalate, that is the thermodynamic product. The preferential carbonate formation was easily explained by the fact that the "key intermediate", a Sm(III)-$(CO_2)^{2-}$-Sm(III) complex, is η^2(C–O) bonded to the Sm centre(s) and therefore favouring O–C rather than C–C bond formation with an incoming CO_2. Recent reports on Ti(III)[23] and Th(III)[3a] chemistry have shown that the donation ability of the ligand can allow the formation of a transient dioxocarbene species that favours the C–C bond formation over the O–C one. In the same way, a seminal work by Tsoureas *et al.* on uranium(III) complexes[24] demonstrated that the carbonate : oxalate ratio can also be tuned by changing the sterics around the metal centres. In all the above studies, only mononuclear complexes were involved in the reaction with CO_2. Experimentally, during the reaction of the dimeric **1-Sm** and **1-Yb** with CO_2, the formation of tetrametallic complexes was observed, which are difficult to handle computationally. A calculation was undertaken on the tetrametallic "key intermediate" $[L_4Sm_2(CO_2)L_4Sm_2]$. The geometry of this complex indicates a dioxocarbene structure that would favour oxalate formation. Moreover, the stabilization of this tetrametallic "key intermediate" with respect to the separated reactants (2 dimers and CO_2) is similar to the one found for the bimetallic intermediate $[L_2Sm(CO_2)L_2Sm]$ formed from the reaction of one dimer and a CO_2.

The carbonate and oxalate formation pathways with **1-Sm** were therefore computed on dimers and are reported in Fig. 5. It should however be kept in mind that the formation of the "key intermediate" from two dimers, although favourable energetically would be disfavoured entropically as it goes from three particles to one with respect to the "key intermediate" formed from one dimer.

The reaction mechanism for the carbonate formation from the reaction of **1-Sm** with CO_2, is classical and similar to previous reports for mononuclear complexes.[3d,9] The formation of the key intermediate is exoergic by 106.2 kcal mol^{-1} and in this compound the CO_2^{2-} moiety is (μ:μ:η(C–O)) bonded to the

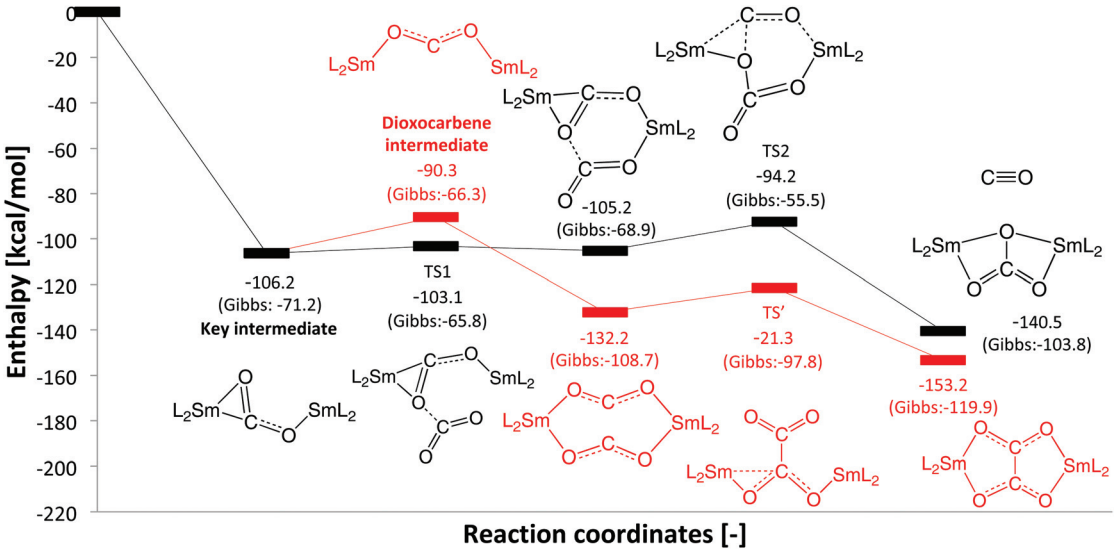

Fig. 5 Computed enthalpy profile (room temperature) for the CO_2 reaction with **1-Sm**. The black profile is the carbonate formation whereas the red one is the oxalate formation pathway.

two samarium centres. No oxo formation is observed in line with the bulkiness of the ligand but a concerted reaction mechanism where the incoming CO_2 forms a C–O bond with the CO_2^{2-} and then releases CO is found. The highest barrier is 12.8 kcal mol^{-1} for the latter and is associated with the need to have the two Sm fragments relatively close increasing the steric repulsion. On the other hand, the formation of the oxalate implies the formation a dioxocarbene intermediate as found with the tetramer. The dioxocarbene intermediate (see Fig. 5) is 15.9 kcal mol^{-1} less stable that the "key intermediate" making this pathway less favourable than the carbonate formation even though the subsequent formation of the CO_2 adduct to the dioxocarbene is highly favourable (−41.9 kcal mol^{-1}). The oxalate formation is then achieved with an equivalent barrier (10.9 kcal mol^{-1}) as the carbonate. This is associated with the formation of a transient dioxocarbene that decreases the steric congestion at the transition state but this intermediate is less stable than the "key intermediate" involved in the carbonate formation. Thus, the formation of the oxalate from the dimer and CO_2 is favoured thermodynamically but kinetics and the formation of tetrametallic intermediate still allow carbonate formation.

Conclusions

In summary we have shown that dinuclear complexes containing low-coordinate lanthanide(II) ions can be stabilized by the polydentate tris(tertbutoxy) siloxide ligand. In spite of the presence of only two siloxide ligands bound to the metal centre the complexes $[Yb_2L_4]$, **1-Yb** and $[Sm_2L_4]$, **1-Sm**, (L = $(O^tBu)_3SiO^-$) are highly reactive as indicated by the observed cleavage of the DME C–O bond over time at room temperature to afford crystals of $[Yb_2L_4(\mu\text{-OMe})_2(DME)_2]$, **2**. More importantly the **1-Yb** and **1-Sm** complexes effect the reduction of CO_2 under ambient conditions leading to both carbonate and oxalate formation. The selectivity of the reduction towards oxalate or carbonate changes depend on the solvent polarity and on the nature of the ion. For both lanthanides, carbonate formation is favoured but oxalate formation increases in non-polar solvents. These results suggest that dimeric species favours oxalate formation. Notably, in non-polar solvents the **1-Yb** and **1-Sm** complexes are present in solution as dimers, while the formation of monomeric species is anticipated in polar solvents. Computational studies confirmed that the formation of oxalate is favoured with respect to carbonate formation in the reaction of the dimeric lanthanide complexes with CO_2. However, the formation of tetrametallic intermediates is likely to result in the concomitant formation of carbonate. Crystals of the tetranuclear mixed-valence oxalate intermediate $[Yb_4L_8(C_2O_4)]$, **3**, were isolated from hexane and the presence of a $C_2O_4^{2-}$ ligand bridging two $[Yb^{II}L_2Yb^{III}L_2]$ dinuclear moieties was shown. Crystals of the tetranuclear di-carbonate product $[Sm_4L_8(\mu_3\text{-}CO_3\text{-}\kappa^4\text{-}O,O',O'')_2]$, **4**, were isolated from hexane. The structures of **3** and **4** suggest that the CO_2 activation in non-polar solvents involves the interaction of two dimers with CO_2 molecules at least to some extent. Such a cooperative interaction results in both oxalate and carbonate formation.

Experimental part

General considerations

Unless otherwise noted, all reactions were performed either using standard Schlenk line techniques or in an inert atmosphere glovebox under an atmosphere of purified argon (<1 ppm O_2/H_2O). Glassware was dried overnight at 150 °C

prior to use. Unless otherwise noted, reagents were acquired from commercial suppliers and used without further purification. The solvents were purchased from Aldrich or Eurisotop (deuterated solvents) in their anhydrous form, conditioned under argon and vacuum distilled from K/benzophenone or Na dispersion/benzophenone (*n*-hexane, toluene, DME, cyclohexane and THF) and degassed prior to use or dried over molecular sieves for one week (DMSO). Syntheses were performed using glass covered stirring bars. $HOSi(OtBu)_3$, and naphthalene were purchased from Aldrich and purified by sublimation prior to use. $[Yb(HMDS)_2(THF)_2]$, $[Sm(HMDS)_2(THF)_2]$,[25] and $[SmL_4K_2]$[8c] (L = $OSi(OtBu)_3$) were prepared using literature procedures. The amount of THF was determined by ^{1}H NMR using naphthalene as the internal reference. NMR experiments were carried out using NMR tubes adapted with J. Young valves. NMR spectra were recorded on Bruker 400 and 600 MHz spectrometers. ^{1}H and ^{13}C chemical shifts are reported in ppm and were measured relative to residual solvent peaks. ^{29}Si NMR chemical shifts are reported in ppm relative to $(TMS)_2O$. Elemental analyses were performed under helium by the analytical service at EPFL. Infrared analyses were performed with a PerkinElmer Frontier FT-IR.

Syntheses

Synthesis of $[Sm_2L_4]$ (1-Sm). A cold (−40 °C) solution of HL (84.6 mg, 0.32 mmol, 2 eq.) in DME (2.5 mL) was added to a stirring solution of $[Sm(HMDS)_2(THF)_2]$ (100 mg, 0.16 mmol, 1 eq.) in DME (1.5 mL). The resulting dark brown solution was stirred overnight at −40 °C. The solvent was removed under vacuum affording a dark brown powder. The solid was dissolved in cold *n*-hexane (3 mL), stirred at −40 °C for 15 min and then dried. This operation was repeated three times to completely remove coordinated DME affording a dark brown solution. Removal of DME by heating under vacuum was avoided because it leads to decomposition. The solution was filtered and concentrated. Storage of the solution at −40 °C yielded dark brown crystals of $[Sm_2L_4]$, **1-Sm** in 74% yield (89 mg, 0.068 mmol). Anal. Calc. for $[Sm_2(OSi(OtBu)_3)_4]$ (1354.4 g mol^{-1}): $C_{48}H_{108}O_{16}Si_4Sm_2$: C, 42.57; H, 8.04. Found: C, 42.45; H, 8.03. ^{1}H NMR (Tol-d_8, 400 MHz, 298 K): δ = 2.80 ppm (s, 108 H). ^{1}H NMR (THF-d_8, 400 MHz, 298 K): δ = 2.07 ppm (s, 108 H). ^{1}H NMR (C_6D_{12}, 400 MHz, 298 K): δ = 2.39 ppm (s), 1.65 ppm (s). Dark brown crystals suitable for X-ray diffraction analysis were obtained from a saturated solution of **1-Sm** in *n*-hexane at −40 °C.

Synthesis of $[Yb_2L_4]$ (1-Yb). A cold (−40 °C) solution of HL (294.9 mg, 1.11 mmol, 2 eq.) in DME (4 mL) was added to a stirring solution of $[Yb(HMDS)_2(THF)_2]$ (355.8 mg, 0.56 mmol, 1 eq.) in DME (2 mL). The resulting orange solution was stirred overnight at −40 °C. The solvent was removed under vacuum affording an orange powder. The solid was dissolved in cold *n*-hexane (3 mL), stirred at −40 °C for 15 min and then dried. This operation was repeated three times affording a dark brown solution to completely remove coordinated DME. The removal of DME by heating under vacuum was avoided because it leads to decomposition. The solution was filtered and concentrated. Storage of the solution at −40 °C yielded green crystals of $[Yb_2L_4]$, **1-Yb** in 81% yield (315 mg, 0.23 mmol). Anal. Calc. for $[Yb_2(OSi(O^tBu)_3)_4]$ (1399.7 g mol^{-1}): $C_{48}H_{108}O_{16}Si_4Yb_2$: C, 41.19; H, 7.78. Found: C, 41.25; H, 7.75. ^{1}H NMR (Tol-d_8, 400 MHz, 298 K): δ = 1.52 ppm (s, 108 H). ^{1}H NMR (THF-d_8, 400 MHz, 298 K): δ = 1.37 ppm (s, 108 H). ^{1}H NMR (C_6D_{12}, 400 MHz, 298 K): δ = 1.47 ppm (s, 108 H). ^{1}H NMR (Tol-d_8, 400 MHz, 213 K): δ = 1.66 ppm, 1.53 ppm. ^{13}C NMR (THF-d_8, 400 MHz, 298 K): δ = 72.13 ppm, 70.35 ppm, 35.52 ppm, 32.63 ppm. ^{13}C NMR (C_6D_{12}, 400 MHz, 298 K): δ = 32.56 ppm. ^{29}Si NMR (THF-d_8, 400 MHz, 298 K): δ = −90.90 ppm.

Stability studies of complexes 1-Yb and 1-Sm

Stability of 1-Yb. The evolution of solutions of **1-Yb** (15 mg, 0.01 mmol) in Tol-d_8 (0.3 mL), THF-d_8 (0.3 mL), and C_6D_{12} (0.3 mL) at room temperature was followed by ^{1}H NMR spectroscopy over time (400 MHz, 298 K). **1-Yb** only shows evidence of decomposition after 36 hours at room temperature in Tol-d_8 and THF-d_8. After 5 days at room temperature, the ^{1}H NMR spectra show a decrease of 15% of the signals of **1-Yb** in Tol-d_8 and THF-d_8. No appearance of new signals was observed over time that could be assigned to the decomposition products. Furthermore, the orange solution of **1-Yb** (30 mg, 0.021 mmol) in DME (0.3 mL) slowly fades over time at room temperature. After 15 days colorless single crystals suitable for X-ray diffraction of $[Yb_2L_4(\mu\text{-}OMe)_2(DME)_2]$ (**2**) could be isolated in a low yield. ^{1}H NMR spectroscopy of **1-Yb** in C_6D_{12} showed that the complex is stable for weeks at room temperature in a C_6D_{12} solution.

Stability of 1-Sm. The evolution of solutions of **1-Sm** (15 mg, 0.01 mmol) in Tol-d_8 (0.3 mL), THF-d_8 (0.3 mL), C_6D_{12} (0.3 mL) at room temperature was followed by ^{1}H NMR spectroscopy over time. **1-Sm** only shows evidence of decomposition after 36 hours at room temperature in THF-d_8. After 5 days at room temperature, the ^{1}H NMR spectra show a decrease of 20% of the signals of **1-Sm** in THF-d_8. No significant new signals were observed over time that could be assigned to the decomposition products. ^{1}H NMR spectroscopy of **1-Sm** in C_6D_{12} showed that the complex is stable for weeks at room temperature in a C_6D_{12} solution. ^{1}H NMR study of **1-Sm** in Tol-d_8 at room temperature showed a decrease of the intensity of the signals assigned to **1-Sm**, reaching 20% of decomposition in Tol-d_8 after 5 days, and the apparition of a signal at δ = 1.08 ppm corresponding to the reduced toluene adduct $[\{Sm_2L_3\}_2(\mu\text{–}\eta^6\text{:}\eta^6\text{-}C_7H_8)]$.[17]

Reactivity

Reactivity of 1-Yb with CO_2 in THF-d_8. $^{13}CO_2$ (~5 equivalents) was added to a liquid nitrogen frozen solution of **1-Yb** (10 mg, 0.007 mmol, 1 eq.) in THF-d_8 (0.3 mL). The solution was allowed to warm up at room temperature resulting in a color change of the solution from orange to yellow. The ^{1}H NMR spectrum of the resulting solution (THF-d_8, 400 MHz, 298 K) shows complete disappearance of the signals of **1-Yb**, the appearance of a signal assigned to the $[YbL_3(THF)_2]$

complex at δ = −16.93 ppm and of a new set of signals at δ = 1.23 ppm, 0.82 ppm and −0.01 ppm. The formation of $[YbL_3(THF)_2]$ increased over 10 days reaching a conversion of approximately 50%, determined by ^{1}H NMR using naphthalene as the internal standard. ^{13}C NMR (THF-d_8, 400 MHz, 298 K): δ = 185.02 ppm (free CO), 169.95 ppm (bound CO_3^{2}), 125.84 ppm (free CO_2), 99.97 ppm (siloxide), 37.67 ppm (siloxide), 31.65 ppm (siloxide) and 10.47 ppm (siloxide). No change in the ^{13}C NMR spectrum is perceived over time. The quantitative ^{13}C NMR of the evaporated reaction mixture after removing the excess of $^{13}CO_2$ in D_2O (D_2O, 600 MHz, 298 K, pD-13) shows a single signal at δ = 168.26 ppm assigned to CO_3^{2-} in 90% yield using ^{13}C-labelled sodium acetate as the internal standard.

Reactivity of 1-Yb with CO_2 in C_6D_{12}. $^{13}CO_2$ (∼5 equivalents) was added to a liquid nitrogen frozen solution of **1-Yb** (10 mg, 0.007 mmol, 1 eq.) in C_6D_{12} (0.3 mL). The solution was allowed to warm up at room temperature resulting in a color change of the solution from dark brown to yellow. The ^{1}H NMR spectrum of the resulting solution (C_6D_{12}, 400 MHz, 298 K) shows signals at δ = 7.31 ppm, 1.54 ppm, 1.47 ppm (**1-Yb**) and 1.41 ppm. After 3 days at room temperature the signals at 1.54 ppm, 1.47 ppm (**1-Yb**) and 1.41 ppm disappeared and two new signals at δ = 1.51 ppm and 1.44 ppm can be identified. The ^{13}C NMR (C_6D_{12}, 400 MHz, 298 K) spectrum of the reaction mixture immediately after the addition of $^{13}CO_2$: δ = 159.2 ppm, 125.82 ppm (free CO_2), 31.77 ppm (siloxide). ^{13}C NMR spectroscopy studies over time (C_6D_{12}, 400 MHz, 298 K) show the continuous decrease of the signal at δ = 159.20 ppm and the complete disappearance of it after 2 weeks at room temperature. The quantitative ^{13}C NMR spectrum of the evaporated reaction mixture after removing the excess of $^{13}CO_2$ in D_2O (D_2O, 600 MHz, 298 K, pD-13) shows two signals at δ = 167.62 ppm assigned to CO_3^{2-} and 179.72 ppm assigned to $C_2O_4^{2-}$ in 94% total yield (oxalate and carbonate, using ^{13}C-labelled sodium acetate as internal standard) with a ratio of 1 : 50 (oxalate : carbonate). Here, the chemical shift of the signal assigned to oxalate is shifted from about 6 ppm compared to free oxalate suggesting that oxalate binding to Yb(III) may still occur at pH = 13. Pale yellow crystals of $[Yb_4L_8(C_2O_4)]$ (**3**) suitable for X-ray diffraction were obtained overnight from a concentrated hexane solution of **1-Yb** at −40 °C after the addition of ∼5 equivalents of CO_2 at room temperature (yield <1%).

Reactivity of 1-Sm with CO_2 in THF-d_8. $^{13}CO_2$ (∼5 equivalents) was added to a liquid nitrogen frozen solution of **1-Sm** (10 mg, 0.007 mmol) in THF-d_8 (0.3 mL). The solution was allowed to warm up at room temperature resulting in a color fading of the solution from dark brown to colorless in few minutes. The ^{1}H NMR spectrum of the resulting solution (THF-d_8, 400 MHz, 298 K) shows the complete disappearance of the signal assigned to **1-Sm** and the formation of signals at δ = 1.51 ppm ($[SmL_3(THF)_2]$) and 1.31 ppm, growing over two days. The quantitative ^{1}H NMR spectrum shows, after two days, a yield of approximately 50%, determined by NMR using naphthalene as the internal standard, for $[SmL_3(THF)_2]$. ^{13}C NMR (THF-d_8, 400 MHz, 298 K); immediately after addition: δ = 185.20 ppm (free CO), 175.86 ppm, 174.43 ppm, 174.21 ppm, 125.94 ppm (free CO_2), 72.37 ppm (siloxide) and 32.97 ppm (siloxide). The quantitative ^{13}C NMR after 10 days of the evaporated reaction mixture after removing the excess of $^{13}CO_2$ in D_2O (D_2O, 600 MHz, 298 K, pD-13) shows two signals at δ = 168.32 ppm assigned to CO_3^{2-} and 173.36 ppm assigned to $C_2O_4^{2-}$ in 90% total yield (oxalate and carbonate, using ^{13}C-labelled sodium acetate as the internal standard) with a ratio of 1 : 104 (oxalate : carbonate).

Reactivity of 1-Sm with CO_2 in C_6D_{12}. $^{13}CO_2$ (∼5 equivalents) was added to a liquid nitrogen frozen solution of **1-Sm** (10 mg, 0.007 mmol) in C_6D_{12} (0.3 mL). The solution was allowed to warm up at room temperature resulting in a color change of the solution from dark brown to light brown. The ^{1}H NMR spectrum of the resulting solution (C_6D_{12}, 400 MHz, 298 K) shows the formation of three sets of peaks at δ = −4.17 ppm, −4.45 ppm and −5.75 ppm. ^{13}C NMR (C_6D_{12}, 400 MHz, 298 K); immediately after addition: δ = 192.43 ppm (bound $C_2O_4^{2-}$/CO_3^{2-}), 191.72 ppm (bound $C_2O_4^{2-}$/CO_3^{2-}), 185.02 ppm (free CO), 128.70 ppm, 125.80 (free CO_2) and 32.14 ppm (siloxide). After 4 days, the color of the solution turned colorless. No change in the ^{1}H NMR spectrum was observed. ^{13}C NMR (C_6D_{12}, 400 MHz, 298 K); after four days at room temperature: δ = 185.02 ppm (free CO), 166.52 ppm, 164.99 ppm, 164.24 ppm, 128.70 ppm, 125.80 (free CO_2) and 32.14 ppm (siloxide). The quantitative ^{13}C NMR of the evaporated reaction mixture after removing the excess of $^{13}CO_2$ in D_2O (D_2O, 600 MHz, 298 K, pD-13) shows signals at 173.25 ppm ($C_2O_4^{2-}$) and 168.31 ppm (CO_3^{2-}) in a 1 : 17 ratio with a total yield of 98% (oxalate and carbonate, using ^{13}C-labelled sodium acetate as the internal standard). Colourless crystals of $[Sm_4L_8(CO_3)_2]$ (**4**) suitable for X-ray diffraction were obtained from a concentrated hexane solution of **1-Sm** left at −40 °C for 2 days after the addition of ∼5 equivalents of CO_2 at room temperature (yield <1%).

Reactivity of $[SmL_4K_2]$ with CO_2 in C_6D_{12}. $^{13}CO_2$ (∼5 equivalents) was added to a liquid nitrogen frozen solution of $[SmL_4K_2]$ (10 mg, 0.008 mmol) in C_6D_{12} (0.3 mL). The solution was allowed to warm up at room temperature resulting in a color change of the solution from red to colorless. The quantitative ^{1}H NMR in C_6D_{12} shows the complete disappearance of the signal assigned to $[SmL_4K_2]$ (δ = 2.41 ppm) and the formation of $[SmL_4K]$ (δ = 0.55 ppm) in approximately 50% yield, determined by NMR using naphthalene as the internal standard. ^{13}C NMR (C_6D_{12}, 400 MHz, 298 K): δ = 202.05 ppm, 198.84 ppm, 168.43 ppm, 157.97 ppm, 156.52 ppm, 156.02 ppm, 125.80 (free CO_2), 72.29 ppm (siloxide), 32.37 ppm (siloxide). ^{1}H NMR and ^{13}C NMR spectroscopy studies did not show any changes in the spectra. The quantitative ^{13}C NMR of the evaporated reaction mixture after removing the excess of $^{13}CO_2$ in D_2O (D_2O, 600 MHz, 298 K, pD-13) shows two signals at δ = 173.36 ppm assigned to $C_2O_4^{2-}$ and δ = 168.22 ppm assigned to CO_3^{2-} in 92% total yield (oxalate and carbonate, using ^{13}C-labelled sodium acetate as the internal standard) with a ratio of 1 : 0.8 (oxalate : carbonate).

Conflicts of interest

There are no conflicts to declare.

Acknowledgements

We acknowledge support from the Swiss National Science Foundation grant number and 200021_178793 and from the Ecole Polytechnique Fédérale de Lausanne (EPFL). We thank Euro Solari for carrying out the elemental analyses, and Rosario Scopelliti for important contributions to the X-ray single crystal structure analyses. We thank Anna Dabrowska and Julie Andrez for preliminary experiments.

Notes and references

1 (*a*) W. B. Tolman, *Activation of Small Molecules: Organometallic and Bioinorganic Perspectives*, Wiley-VCH, Verlag, 2006; (*b*) C. Finn, S. Schnittger, L. J. Yellowlees and J. B. Love, *Chem. Commun.*, 2012, **48**, 1392–1399; (*c*) E. E. Benson, C. P. Kubiak, A. J. Sathrum and J. M. Smieja, *Chem. Soc. Rev.*, 2009, **38**, 89–99; (*d*) K. Huang, C. L. Sun and Z. J. Shi, *Chem. Soc. Rev.*, 2011, **40**, 2435–2452; (*e*) M. Aresta and A. Dibenedetto, *J. Chem. Soc., Dalton Trans.*, 2007, 2975–2992; (*f*) M. Aresta, *Carbon Dioxide as a Chemical Feedstock*, Wiley VCH, 2010.

2 (*a*) K. A. Grice, *Coord. Chem. Rev.*, 2017, **336**, 78–95; (*b*) P. L. Arnold and Z. R. Turner, *Nat. Rev. Chem.*, 2017, **1**, 0002.

3 (*a*) A. Formanuik, F. Ortu, C. J. Inman, A. Kerridge, L. Castro, L. Maron and D. P. Mills, *Chem. – Eur. J.*, 2016, **22**, 17976–17979; (*b*) O. P. Lam and K. Meyer, *Polyhedron*, 2012, **32**, 1–9; (*c*) I. Castro-Rodriguez and K. Meyer, *Chem. Commun.*, 2006, 1353–1368; (*d*) N. W. Davies, A. S. P. Frey, M. G. Gardiner and J. Wang, *Chem. Commun.*, 2006, 4853–4855; (*e*) G. B. Deacon, P. C. Junk, J. Wang and D. Werner, *Inorg. Chem.*, 2014, **53**, 12553–12563; (*f*) D. Heitmann, C. Jones, D. P. Mills and A. Stasch, *J. Chem. Soc., Dalton Trans.*, 2010, **39**, 1877–1882; (*g*) I. Castro-Rodriguez, H. Nakai, L. N. Zakharov, A. L. Rheingold and K. Meyer, *Science*, 2004, **305**, 1757–1759; (*h*) L. Castro, S. Labouille, D. R. Kindra, J. W. Ziller, F. Nief, W. J. Evans and L. Maron, *Chem. – Eur. J.*, 2012, **18**, 7886–7895; (*i*) L. Castro and L. Maron, *Chem. – Eur. J.*, 2012, **18**, 6610–6615; (*j*) O. P. Lam, L. Castro, B. Kosog, F. W. Heinemann, L. Maron and K. Meyer, *Inorg. Chem.*, 2012, **51**, 781–783; (*k*) J. G. Brennan, R. A. Andersen and A. Zalkin, *Inorg. Chem.*, 1986, **25**, 1756–1760; (*l*) L. Castro, O. P. Lam, S. C. Bart, K. Meyer and L. Maron, *Organometallics*, 2010, **29**, 5504–5510; (*m*) I. Castro-Rodriguez and K. Meyer, *J. Am. Chem. Soc.*, 2005, **127**, 11242–11243; (*n*) L. Castro, D. P. Mills, C. Jones and L. Maron, *Eur. J. Inorg. Chem.*, 2016, 792–796.

4 (*a*) A. C. Schmidt, A. V. Nizovtsev, A. Scheurer, F. W. Heinemann and K. Meyer, *Chem. Commun.*, 2012, **48**, 8634–8636; (*b*) I. Korobkov and S. Gambarotta, in *Progress in Inorganic Chemistry*, ed. K. D. Karlin, 2005, vol. 54, pp. 321–348; (*c*) B. M. Gardner and S. T. Liddle, *Eur. J. Inorg. Chem.*, 2013, **2013**, 3753–3770; (*d*) O. T. Summerscales and F. G. N. Cloke, *Organometallic and Coordination Chemistry of the Actinides*, 2008, vol. 127, pp. 87–117; (*e*) H. S. La Pierre and K. Meyer, in *Prog. Inorg. Chem*, ed. K. D. Karlin, 2014, vol. 58, pp. 303–415; (*f*) S. T. Liddle, *Angew. Chem., Int. Ed.*, 2015, **54**, 8604–8641; (*g*) R. J. Kahan, F. G. N. Cloke, S. M. Roe and F. Nief, *New J. Chem.*, 2015, **39**, 7602–7607; (*h*) C. J. Inman, A. S. P. Frey, A. F. R. Kilpatrick, F. G. N. Cloke and S. M. Roe, *Organometallics*, 2017, **36**, 4539–4545; (*i*) C. L. Webster, J. W. Ziller and W. J. Evans, *Organometallics*, 2013, **32**, 4820–4827; (*j*) W. J. Evans, C. A. Seibel and J. W. Ziller, *Inorg. Chem.*, 1998, **37**, 770–776.

5 (*a*) A. S. P. Frey, F. G. N. Cloke, M. P. Coles, L. Maron and T. Davin, *Angew. Chem., Int. Ed.*, 2011, **50**, 6881–6883; (*b*) O. T. Summerscales, F. G. N. Cloke, P. B. Hitchcock, J. C. Green and N. Hazari, *J. Am. Chem. Soc.*, 2006, **128**, 9602–9603; (*c*) O. T. Summerscales, F. G. N. Cloke, P. B. Hitchcock, J. C. Green and N. Hazari, *Science*, 2006, **311**, 829–831; (*d*) B. M. Gardner, J. C. Stewart, A. L. Davis, J. McMaster, W. Lewis, A. J. Blake and S. T. Liddle, *Proc. Natl. Acad. Sci. U. S. A.*, 2012, **109**, 9265–9270; (*e*) P. L. Arnold, Z. R. Turner, R. M. Bellabarba and R. P. Tooze, *Chem. Sci.*, 2011, **2**, 77–79; (*f*) V. Mougel, C. Camp, J. Pecaut, C. Coperet, L. Maron, C. E. Kefalidis and M. Mazzanti, *Angew. Chem., Int. Ed.*, 2012, **51**, 12280–12284; (*g*) O. Cooper, C. Camp, J. Pécaut, C. E. Kefalidis, L. Maron, S. Gambarelli and M. Mazzanti, *J. Am. Chem. Soc.*, 2014, **136**, 6716–6723; (*h*) C. Camp, O. Cooper, J. Andrez, J. Pecaut and M. Mazzanti, *J. Chem. Soc., Dalton Trans.*, 2015, **44**, 2650–2656.

6 W. J. Evans, J. M. Perotti, J. C. Brady and J. W. Ziller, *J. Am. Chem. Soc.*, 2003, **125**, 5204–5212.

7 (*a*) U. R. Pokharel, F. R. Fronczek and A. W. Maverick, *Nat. Commun.*, 2014, **5**, 5883; (*b*) R. Angamuthu, P. Byers, M. Lutz, A. L. Spek and E. Bouwman, *Science*, 2010, **327**, 313–315; (*c*) C. T. Saouma, C. C. Lu, M. W. Day and J. C. Peters, *Chem. Sci.*, 2013, **4**, 4042–4051; (*d*) L. J. Farrugia, S. Lopinski, P. A. Lovatt and R. D. Peacock, *Inorg. Chem.*, 2001, **40**, 558–559; (*e*) C. C. Lu, C. T. Saouma, M. W. Day and J. C. Peters, *J. Am. Chem. Soc.*, 2007, **129**, 4–5.

8 (*a*) W. J. Evans, S. E. Lorenz and J. W. Ziller, *Inorg. Chem.*, 2009, **48**, 2001–2009; (*b*) N. Tsoureas, A. F. R. Kilpatrick, C. J. Inman and F. G. N. Cloke, *Chem. Sci.*, 2016, **7**, 4624–4632; (*c*) J. Andrez, J. Pecaut, P.-A. Bayle and M. Mazzanti, *Angew. Chem., Int. Ed.*, 2014, **53**, 10448–10452; (*d*) A.-C. Schmidt, F. W. Heinemann, C. E. Kefalidis, L. Maron, P. W. Roesky and K. Meyer, *Chem. – Eur. J.*, 2014, **20**, 13501–13506.

9 M. Xemard, V. Goudy, A. Braun, M. Tricoire, M. Cordier, L. Ricard, L. Castro, E. Louyriac, C. E. Kefalidis, C. Clavaguera, L. Maron and G. Nocton, *Organometallics*, 2017, **36**, 4660–4668.

10 (*a*) G. Fachinetti, C. Floriani and P. F. Zanazzi, *J. Am. Chem. Soc.*, 1978, **100**, 7405–7407; (*b*) S. Gambarotta, F. Arena, C. Floriani and P. F. Zanazzi, *J. Am. Chem. Soc.*, 1982, **104**, 5082–5092.

11 (*a*) J. P. Krogman, B. M. Foxman and C. M. Thomas, *J. Am. Chem. Soc.*, 2011, **133**, 14582–14585; (*b*) J. H. Jeoung and H. Dobbek, *Science*, 2007, **318**, 1461–1464.

12 (*a*) W. J. Evans, N. T. Allen and J. W. Ziller, *J. Am. Chem. Soc.*, 2001, **123**, 7927–7928; (*b*) W. J. Evans, G. Zucchi and J. W. Ziller, *J. Am. Chem. Soc.*, 2003, **125**, 10–11; (*c*) W. J. Evans, K. A. Miller and J. W. Ziller, *Angew. Chem., Int. Ed.*, 2008, **47**, 589–592; (*d*) O. P. Lam, S. C. Bart, H. Kameo, F. W. Heinemann and K. Meyer, *Chem. Commun.*, 2010, **46**, 3137–3139; (*e*) W. J. Evans, *J. Alloys Compd.*, 2009, **488**, 493–510.

13 (*a*) A. S. P. Frey, F. G. N. Cloke, M. P. Coles and P. B. Hitchcock, *Chem. – Eur. J.*, 2010, **16**, 9446–9448; (*b*) O. T. Summerscales, A. S. P. Frey, F. Geoffrey, N. Cloke and P. B. Hitchcock, *Chem. Commun.*, 2009, 198–200; (*c*) S. M. Mansell, N. Kaltsoyannis and P. L. Arnold, *J. Am. Chem. Soc.*, 2011, **133**, 9036–9051; (*d*) W. J. Evans, J. W. Grate, I. Bloom, W. E. Hunter and J. L. Atwood, *J. Am. Chem. Soc.*, 1985, **107**, 405–409.

14 E. Louyriac, P. W. Roesky and L. Maron, *J. Chem. Soc., Dalton Trans.*, 2017, **46**, 7660–7663.

15 (*a*) M. Falcone, L. Barluzzi, J. Andrez, F. F. Tirani, I. Zivkovic, A. Fabrizio, C. Corminboeuf, K. Severin and M. Mazzanti, *Nat. Chem.*, 2019, **11**, 154–160; (*b*) M. Falcone, L. Chatelain, R. Scopelliti, I. Zivkovic and M. Mazzanti, *Nature*, 2017, **547**, 332–335; (*c*) P. L. Arnold, C. J. Stevens, N. L. Bell, R. M. Lord, J. M. Goldberg, G. S. Nichol and J. B. Love, *Chem. Sci.*, 2017, **8**, 3609–3617; (*d*) M. Xemard, M. Cordier, E. Louyriac, L. Maron, C. Clavaguera and G. Nocton, *J. Chem. Soc., Dalton Trans.*, 2018, **47**, 9226–9230.

16 W. J. Evans, D. S. Lee, D. B. Rego, J. M. Perotti, S. A. Kozimor, E. K. Moore and J. W. Ziller, *J. Am. Chem. Soc.*, 2004, **126**, 14574–14582.

17 R. P. Kelly, D. Toniolo, F. F. Tirani, L. Maron and M. Mazzanti, *Chem. Commun.*, 2018, **54**, 10268–10271.

18 G. Lapadula, M. P. Conley, C. Coperet and R. A. Andersen, *Organometallics*, 2015, **34**, 2271–2277.

19 (*a*) D. J. Duncalf, P. B. Hitchcock and G. A. Lawless, *Chem. Commun.*, 1996, 269–271; (*b*) G. B. Deacon, P. C. Junk and G. J. Moxey, *Z. Anorg. Allg. Chem.*, 2008, **634**, 2789–2792; (*c*) G. B. Deacon, C. M. Forsyth and N. M. Scott, *Eur. J. Inorg. Chem.*, 2000, 2501–2506.

20 E. Prasad, B. W. Knettle and R. A. Flowers, *J. Am. Chem. Soc.*, 2002, **124**, 14663–14667.

21 C. Camp, J. Pecaut and M. Mazzanti, *J. Am. Chem. Soc.*, 2013, **135**, 12101–12111.

22 M. Nishiura, Z. M. Hou and Y. Wakatsuki, *Organometallics*, 2004, **23**, 1359–1368.

23 A. Paparo, J. S. Silvia, C. E. Kefalidis, T. P. Spaniol, L. Maron, J. Okuda and C. C. Cummins, *Angew. Chem., Int. Ed.*, 2015, **54**, 9115–9119.

24 N. Tsoureas, L. Castro, A. F. R. Kilpatrick, F. G. N. Cloke and L. Maron, *Chem. Sci.*, 2014, **5**, 3777–3788.

25 W. J. Evans, D. K. Drummond, H. M. Zhang and J. L. Atwood, *Inorg. Chem.*, 1988, **27**, 575–579.